

Influence of the optical parameters of the quantum well solar cells upon conversion efficiency

S. FARA^{a*}, P. STERIAN^a, L. FARA^a, M. IANCU

IPA SA Bucharest, Romania

^aAcademic Center for Optical Engineering and Photonics, Faculty of Applied Sciences, University "Politehnica" Bucharest, Romania

Quantum Well (QW) Photovoltaic Cells - third generation solar cells, were proposed in 1990 by the research group of Professor Keith Barnham, aiming at extending the spectral response and at increasing the photocurrent. This paper tackles some original aspects regarding the influence of the optical parameters of the quantum well solar cells, upon conversion efficiency, based on the modelling and simulation approach, as follows:

- Refraction index modelling and simulation;
- Reflectance modelling and simulation;
- Absorption coefficient modelling;

Evaluation of datasheet parameters of the multiple quantum well solar cells (MQW); our study is based on the hybrid model HM which allows computing of the levels whatsoever the form of the quantum wells.

(Received December 15, 2009; accepted January 20, 2010)

Keyword: MWQ, Reflectance, Refraction index, Absorption, Conversion efficiency

1. Introduction

In 2006-2008 the CEEX project "Research concerning increase in the efficiency of nanostructured solar-cells" – NANO-PV was achieved by the research groups from three universities (Polytechnic University of Bucharest, Timisoara West University, and Polytechnic University of Timisoara) under the coordination of IPA SA. Inside of this project was developed the concept of solar cell quantum well proposed by Keith Barnham [1].

The high research has acted for modelling, simulation and evaluation of the solar cells from the third generation, which allow obtaining a high efficient solar cell at low cost. There are three options for such cells, all based on using nanotechnologies.

Photovoltaic cells are the diodes in which, after lighting, are generated electron-gap pairs that reduces the junction potential, causing a photovoltaic potential. The generating of pairs is described by ambipolar diffusion equation [2]

$$\Delta n(z, T) = \Delta p(z, T) = \frac{G\tau L_D^2}{L_D^2 - L_\lambda^2} \left[\frac{L_\lambda^2}{L_D^2} \exp\left(-\frac{z}{L_\lambda}\right) + \left(1 - 2\frac{L_\lambda^2}{L_D^2}\right) \frac{\sinh\left(\frac{l-z}{L_D}\right)}{\sinh\left(\frac{l}{L_D}\right)} - \frac{L_\lambda^2}{L_D^2} \exp\left(-\frac{l}{L_\lambda}\right) \frac{\sinh\left(\frac{z}{L_D}\right)}{\sinh\left(\frac{l}{L_D}\right)} \right] \quad (1)$$

where $\Delta n(z, T)$ and $\Delta p(z, T)$ are the concentration of non-equilibrium carriers photo-generator at depth z from the illuminated surface, G is the rate of photo-generation, τ is the lifetime of the unbalanced carriers, L_D is the ambipolar diffusion length, L_λ depth of radiation with wavelength λ penetration and l the thickness of the illuminated sample. How carriers have different mobility (e.g., in silicon, mobility gaps is approximately three times higher than that of electrons), the majority from the surface of the sample will be the non-equilibrium carriers with little mobility and at the bottom the majority will be represented by those with high mobility. Accordingly, the diode must be oriented so that the photovoltaic potential to oppose the junction potential (in the silicon example, with n area at the surface and p area at the bottom). Photovoltaic cells of "quantum well" are a particular case of photovoltaic cells [3], which are using the special benefits of systems with

reduced dimension, where at least one of the dimensions is of nanometer order. Because of this the quantum confinement effects were introduced and the role of surface/interface was raised (the surface/volume is of the order $1/d \sim 10^8 \text{ m}^{-1}$, d is the minimum size). Note that if the dimensions are under about 5nm (about 20 interatomic distances), the role of the material chosen become secondary after the confinement. As a result, cells are classified after dimension in 2D, 1D, 0D and fractal cells.

The quantum well cell (QW) is a p-i-n structure having quantum wells built in the intrinsic. Doped regions on each side will produce an electric field perpendicular to the layers of quantum wells. It is also possible to have induced electric fields, because of the piezoelectric effects. These fields are induced by the intensities from the semiconductor layers, because of the disparity between network constants [4].

The multiple quantum well solar cells (MQW) is a system that contains a layer in which the carrier assemblies comply quantum rules in connection with layers in which the carrier assemblies are performing classical, and its modelling is conducted on two dimensional levels [5]:

1. Quantum level in which in which one computes the energy spectrum of the electron and the absorption coefficient of the MQW;

2. Macroscopic level in which one studies the transport of charge carriers in a similar manner to the conventional p-i-n diode. The reflection of light is brought considering MQW cell a pseudo-homogeneous medium.

This combination of quantum and classical elements used in modelling of MQW solar cell justifies the name of hybrid given to the model of MQW solar cell. An example of application of this hybrid model (HM) [6] is the case of solar cell based on a ternary alloy semiconductor $A_xB_{1-x}C$ ($Al_xGa_{1-x}As/GaAs$) which has the lowest BC band gap = 0) and achieve the greatest value ($x = 1$) for the AC semi conductor band gap.

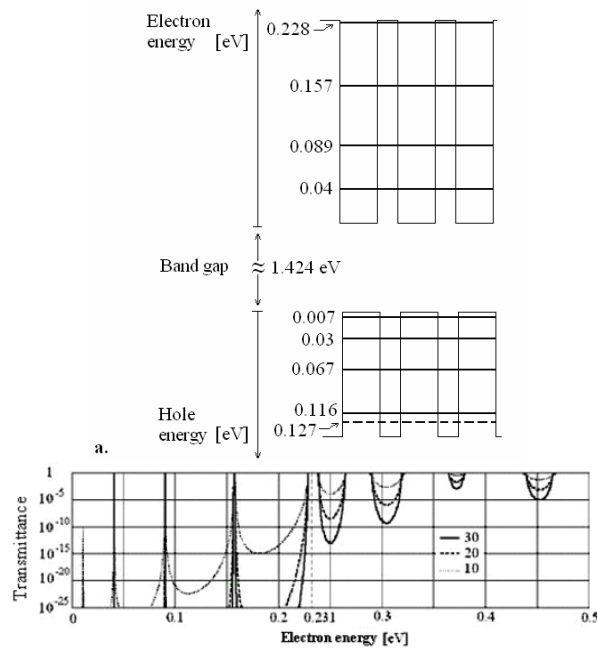


Fig. 1. (a) Schematic representation of levels in the valence bands and conduction for the MQW system $Al_{0.3}Ga_{0.7}As/GaAs$ containing 30 quantum wells. The corresponding level for the heavy gaps it's made with dotted line. (b) Transmission coefficient based on the electron energy for the same system. The curves parameter is the number of quantum wells.

In Fig. 1 are graphically represented the transmittances and energetic levels in the MWQ system as a result of the transport matrix algorithm [7]. The proper values from Figure 1a and resonances from Fig. 1 (b) are identical and mutually confirmed. The levels represented in Figure 1a are obtained by applying Kramer's rule while

the transmittances represented in Fig. 1 (b) are calculated via the transfer matrix. It is noted that a large variation of alloy composition x doesn't determine significant changes in position of the first level from the quantum wells, which means that there is a weak dependence between short circuit current and the ternary alloy composition. Each curve in Figure 1b is calculated in 104 point in less than a minute.

We proposed in this paper to explore possibilities for increasing the conversion efficiency of MQW solar cells and reduce losses by optimizing the optical characteristics (refraction index, the reflectance, the absorbance). Results are summarized in the CEEX grant no. 247, based essentially on the development of the HM hybrid model of the solar cells with quantum wells.

2. Modelling and simulation of refraction index and reflectance

Investigation of electric field effects on the **refraction index** of MQW solar cells can be achieved by calculating the absorption coefficient [8]. In the case of solar cells with quantum wells was introduced the hypothesis of an electrostatic field generated by the load regions. For this reason, it is expected a non-varying change in the refraction index. Based on the results obtained by Barnham [9], it should be noted that the quantum wells from the solar cells of this type are designed to use the spectrum region, with the possibility of generating particles in those quantum wells. For the refraction index of the solar cell with quantum wells it was used the following expression:

$$n = \sqrt{1 + \frac{E_d}{E_o} + \frac{E_d}{E_o^3} E^2 + \frac{\eta}{\pi} E^4 \ln \left(\frac{2E_o^2 - E_g^2 - E^2}{E_r^2 - E^2} \right)} \quad (2)$$

The parameters are: $E_g = 1.6729$; $E_r = 1.4235$; $E_o = 2.6 + 0.7E_r$; $E_d = F/E_o$ and η can be: $\eta = \frac{\pi E_d}{2E_o^3(E_o^2 - E_r^2)}$ The

simulation results for the refraction index depending on the photon energy are represented in Fig. 2.

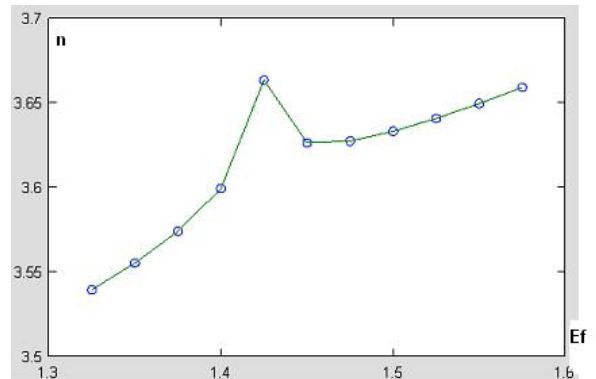


Fig. 2. The refraction index of the cells with quantum wells depending on the photon energy.

The index of refraction model can be used to explore the relation between the index of refraction and reflectance. To achieve this, the refraction index model must be combined with the Fresnel relations, thus allowing the finding the losses caused by reflection of the quantum wells structure. The R reflectance of the solar cell can be calculated using a Fresnel-type relation [10].

$$R = \frac{r_1^2 + r_2^2 + 2r_1r_2 \cos 2\theta}{1 + r_1^2 r_2^2 + 2r_1r_2 \cos 2\theta} \quad (3)$$

$$\text{where } r_1 = \frac{n_0 - n_1}{n_0 + n_1}; r_2 = \frac{n_1 - n_2}{n_1 + n_2}; \theta = \frac{2\pi n_1 d_1}{\lambda} \quad (4)$$

The following notations were introduced:

- n_0 the refraction index of the incident environment; for air $n_0 = 1$;
- n_1 the refraction index of the anti reflecting coating;
- n_2 the refraction index of the under layer (the solar cell with quantum wells);

Thickness d_1 of the anti reflecting coating can be determined by minimizing the last relation (4). It was noted that this value is approximately 600-650nm, for the minimum reflection.

It can be evaluated the effect of the quantum well number on the index of refraction and on the reflection losses so the optimal number of the quantum well for the structure could be calculated.

In Fig. 3 are the results of the optical simulation of solar cells with quantum well (based on relations (3) – (4) and on the model analyzed for the refraction index by relation (2)), in the form of dependence on reflectance R , depending on the wavelength for different thicknesses d for the anti reflecting coating; were considered two cases of anti reflecting coating ($n_1 = 2.4$ – TiO₂ and $n_1 = 1.4$ – SiO). Results from model are consistent with experimental results obtained. The reflectance model can be used to determine the variation effects of quantum well number on the index of refraction.

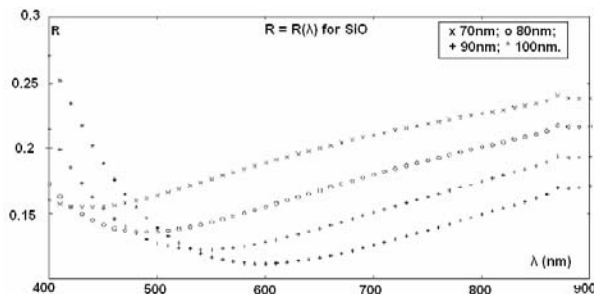


Fig. 3. Simulation of the reflectance for a solar cell with QW structure, for a SiO anti reflecting coating.

The simulation of refraction index and reflectance of the solar cells with quantum wells have been made with the Octave software, version 3.02.

The cell reflectance can be calculated using the refraction indices of GaAs semi conductor and of the Al_{0.3}Ga_{0.7}As alloy (obtained by filtering the experimental data [11]).

$$n_{GaAs}(\lambda) = \begin{cases} \text{if } 0.325 < \lambda \leq 4: \\ \frac{3.24123 - \frac{4.8304085}{\lambda} + \frac{2.82482}{\lambda^2} - \frac{0.769037}{\lambda^3} + \frac{0.08198}{\lambda^4}}{1 - \frac{1.5308}{\lambda} + \frac{0.9123972}{\lambda^2} - \frac{0.2508648}{\lambda^3} + \frac{0.026769}{\lambda^4}} \\ \text{if } 0.2 \leq \lambda \leq 0.325: \\ \frac{2.8434068 - \frac{1.8916996}{\lambda} + \frac{0.4189801}{\lambda^2} - \frac{0.0308637}{\lambda^3}}{1 - \frac{0.682372}{\lambda} + \frac{0.154593}{\lambda^2} - \frac{0.01159}{\lambda^3}} \end{cases} \quad (5)$$

In equation (5) λ is expressed in μm . The refraction index of ternary alloy Al_xGa_{1-x}As is calculated using the same translation procedure of the axes as in the case of the absorption coefficient:

$$n_{Al_xGa_{1-x}As}(\lambda) = [1.05 - 0.53x + 0.09x^2] n_{GaAs}(\lambda_x) \quad (6)$$

with λ in μm .

To minimize the reflection losses the solar cells are frequently coated with anti reflecting coating -ARC.

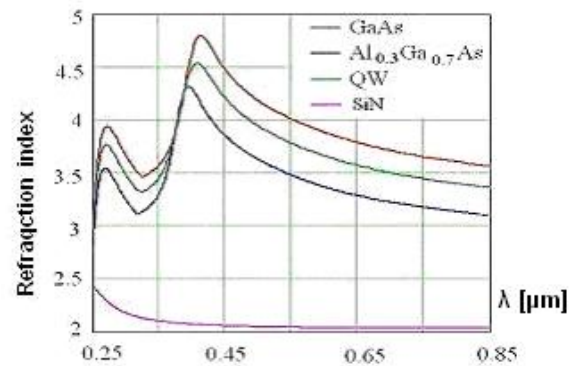


Fig. 4. The refraction index for the materials involved in constructing a MQW cell.

In Fig. 4 are the values calculated for the four refraction indices listed according the wavelength. The MQW layer was considered to consist of 30 quantum wells of GaAs of 20 nm width separated by barriers Al_{0.3}Ga_{0.7}As with width of 10 nm. SiN is the ARC transparent material.

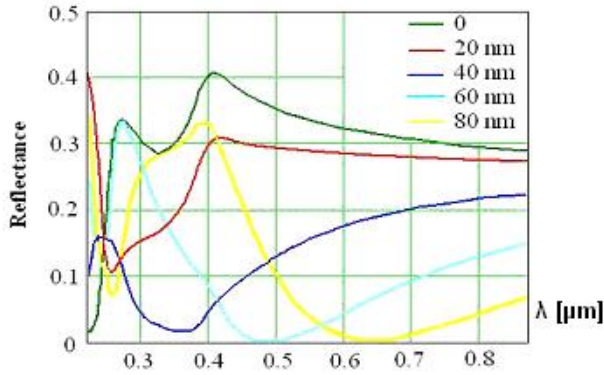


Fig. 5. Spectral reflectance of the MQW cell for different width (in nanometer) of the anti reflecting coating. The HM model was run for GaAs/Al_{0.3}Ga_{0.7}As with $N_w = 30$, $l_w = 20\text{nm}$ and $l_b = 10\text{nm}$.

In Fig. 5 are summarized the results of reflection losses for the various thicknesses of the anti reflecting coating. In the absence of ARC, reflection is an important mechanism of losses exceeding 30% on the spectral range in which the cell absorbs. The other curves show that it is possible to reduce losses through reflection by covering with an anti reflecting coating of appropriate thickness.

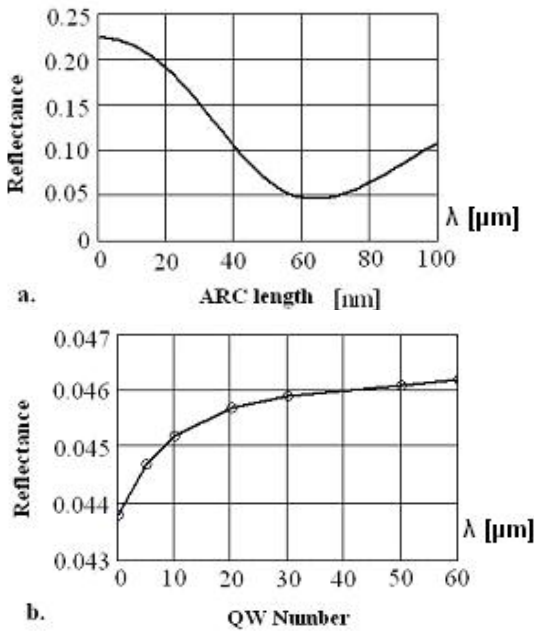


Fig. 6. (a). ARC length influence over the cell reflectance; (b). Influence of the number of quantum wells over the cell reflectance. The HM model was run for GaAs/Al_{0.3}Ga_{0.7}As with $N_w = 30$, $l_w = 20\text{ nm}$ and $l_b = 10\text{ nm}$.

In Fig. 6 (a) the reflectance of the cell is graphically represented. It was obtained by the summary of all wave

lengths of the spectral reflectance from Fig. 6. For considered materials the minimum value of the reflectance is 4.6% obtained for an ARC thickness of 64nm. Contrary to expectations Fig. 6 (b) shows only a slight increase in cell reflectance along with increasing the number of interfaces, as a result of multiple reflection processes [12].

3. Modelling and simulation of absorption coefficient

In applications related to calculating the conversion efficiency of solar cells, but also in other applications, the coefficient of absorption (the absorbance) is practically described by continuous functions. For GaAs, dropping from the experimental data [13] was determined the following function that approximates the acceptable rate of absorption:

$$\alpha_{\text{GaAs}}(\lambda) = \begin{cases} e^{y_1(\lambda)}, & 0.7 < \lambda \leq 0.88 \\ e^{y_2(\lambda)}, & 0.24 < \lambda \leq 0.7 \\ e^{y_2(0.24)}, & 0 < \lambda \leq 0.24 \\ 0, & \text{otherwise} \end{cases} \quad (7)$$

$$y_1(\lambda) = -0.7863 + 5.3115 \left[1 + \operatorname{erf} \left(-\frac{\lambda - 0.84291}{0.038} \right) \right] \quad (8a)$$

$$y_2(\lambda) = -447.432 + 4201.2\lambda^2 + 6835.128\lambda^2 \ln \lambda - 3781.193\lambda^3 + \frac{3.9049}{\lambda^2} \quad (8b)$$

In Fig. 7 is graphically represented the absorption coefficient for GaAs calculated with the algorithm from [14] for different compositions of the alloy.

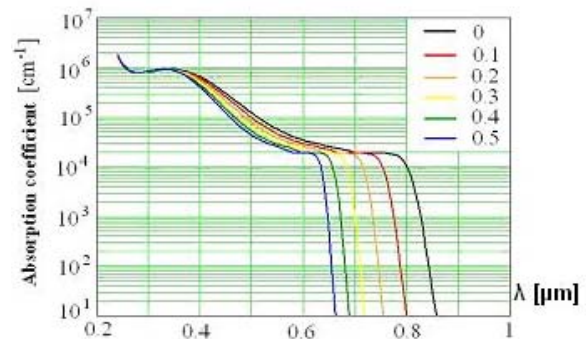


Fig. 7. Absorption coefficient of Al_xGa_{1-x}As depending on wavelength; x is the curves parameter.

In Fig. 8 are graphically compared the absorption coefficients for GaAs, Al_{0.5}Ga_{0.5}As and MQW system. It is noted that with increasing energy the absorption

coefficient from MQW system increases in steps, this is because of the quantifying of the density of states in confinement of the carriers' direction.

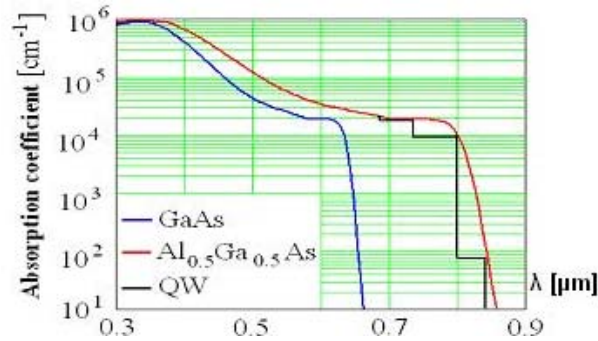


Fig. 8. The absorption coefficient in GaAs crystal, the ternary compound $Al_{0.5}Ga_{0.5}As$ is calculated using axes translation in MQW system.

Absorption coefficient $\alpha_x(\lambda)$ of the $Al_xGa_{1-x}As$ alloy is generated from the absorption coefficient of the GaAs

$$\alpha_0(\lambda):$$

$$\alpha_x(\lambda) = \alpha_0(\lambda_x) \quad (9)$$

$$\lambda_x = \frac{hc}{\frac{hc}{\lambda} - E_g(x) + E_g(0) + a \left[\frac{hc}{\lambda} - E_g(0) \right]^b} \quad (10)$$

where h is Planck constant, c is the speed of light, $a = 0.62$ and $b = 0.5$ [14].

4. Increasing conversion efficiency of the MQW solar cells

The HM model may have the capability to evaluate the performances of the MQW cell. These are represented by the shape factor of cell:

$$F_f = \frac{V_m I_m}{V_{CD} I_{SC}} \quad (11)$$

and conversion efficiency

$$\eta = \frac{V_m I_m}{\int G_0(\lambda) d\lambda} \quad (12)$$

where V_m and I_m are the operation point coordinates when the power supplied in the load is maximum [15].

In Fig. 9, for the cell parameters $N_w = 30$, $l_w = 20$ nm and $l_b = 10$ nm are summarized the calculation results of the conversion efficiency. In Fig. 9 (a) are represented the current-intensity characteristic with the power dissipated by the cell in the external circuit. Hence the main

parameters of the cell are: $J_{SC} = 48.5$ mA/cm², $V_{CD} = 0.886$ V, $F_f = 0.86$ and $\eta = 0.371$. The numerical values are closed to those reported in literature. As for the conventional cell with a p-n junction the maximum possible efficiency is estimated at 34% [15] the result nor confirms nor invalidates that the insertion of MQW in the space-load region improves the conversion efficiency. Fig. 9 (b) shows the conversion efficiency dependence on the anti reflecting coating depth. It can be noted that in the ideal case, when the cell reflectance is neglected, the MQW cell efficiency based on GaAs/ $Al_xGa_{1-x}As$ doesn't exceeds 40%. Unlike the reflectance, in Fig. 9c it is observed that the conversion efficiency is strongly correlated with the number of quantum wells up to $N_w = 30$; Over this value the efficiency is saturated in proportion to N_w . This is a consequence of the way the light takes inside the MQW system; saturation is installed when the road length travelled by the light is comparable to the absorption length.

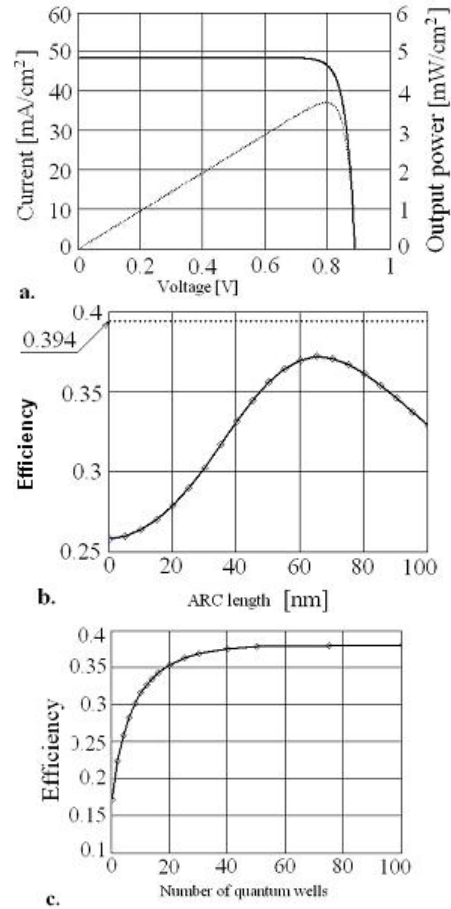


Fig. 9. (a) Voltage-current characteristic (line) and the output power (points) of the cell with the following MQW system: GaAs/ $Al_{0.3}Ga_{0.7}As$, $N_w = 30$, $l_w = 20$ nm, $l_b = 10$ nm and the anti reflecting coating depth $d = 64$ nm. (b) The MQW cell efficiency depending on the anti reflecting coating depth. The dotted line indicates the ideal cell efficiency with zero reflectance. (c) The efficiency of MQW cell based on the number of quantum wells.

This is a one way to use the HM model. Knowing the materials of which it consist MQW cell and optoelectronic properties of these, for a given geometric configuration it can be calculated the conversion efficiency. Obviously the calculation can be repeated varying different geometrical and material parameters in order to determine the optimal configuration, i.e. one that maximizes efficiency.

There is also another way to use HM starting from the assumption that a certain levels structure in MQW system exists. In the next example we consider that in each valence and conduction band are 3 levels and the system has an effective width of the band gap $E_{gw} = 1.1E_{g0}$.

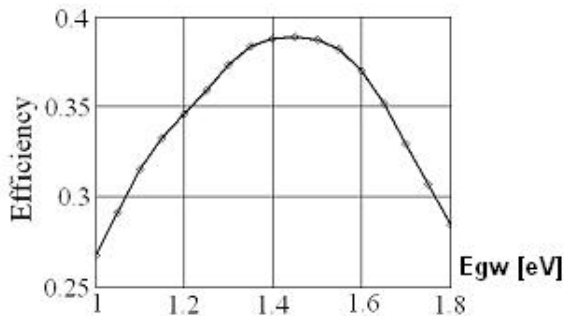


Fig. 10. The MQW cell efficiency depending on the width of the band gap of the material in which are located the quantum wells.

In Fig. 10 there is a performance evaluation of the MQW solar cells efficiency is revealed in which the presumptive levels system is subject to optimization. The cell reflectance was considered 4% across the spectral range and the absorption coefficient is given by relation [16]:

$$\alpha(\lambda, E_{G0}) = \begin{cases} 10^5 \left(\frac{1.24}{\lambda \cdot E_{G0}} - 1 \right)^{1/2} & \text{if } 0.2 \leq \lambda < \frac{1.24}{E_{G0}} \\ 0 & \text{otherwise} \end{cases} \quad (13)$$

5. Conclusions

The results were based on using HM hybrid model of the MQW solar cells, after simulation the simulation highlighted the following conclusions:

- It could be evaluate the quantum well number effect over the refraction index and reflection losses by determine the quantum well optimal number of the structure;
- The reflectance model proposed by authors could be used to determine variation effect of the quantum well number over the refraction index;
- It was developed an absorption coefficient model which was used for study the simulation of the MQW solar cells in special weather conditions;

- The results generated by the model simulator agree with the experimental ones [7]

There has been studied a number of MQW solar cells configurations for optimized values of the optical parameters (reflectance, refraction index, absorption), so the conversion efficiency to be improved.

Acknowledgements

The results of this paper are based on the CEEEX grant no. 247/09.2006, NANO-PV. We would like to acknowledge and thank our collaborators from the University Politehnica of Bucharest, the West University of Timisoara and the University Politehnica of Timisoara for the good and fruitful collaboration in developing the NANO-PV project.

References

- [1] K. Barnham, G. Duggan, Appl. Phys. **67**, 3490 (1990).
- [2] J. Connolly, PhD. Thesis, Imperial College of Science, Technology and Medicine, University of London, 1997.
- [3] Technical Report of Phase IV NANO_PV-Research concerning increase in the efficiency of nanostructured solar-cells, Excellence Research National Programme, 2008.
- [4] K. Barnham, 11th E. C. Photovoltaic Solar Energy Conference, Montreux, Switzerland, 146, 1992.
- [5] A. Goetzberger, J. Knobloch, B. Voss, Crystalline Silicon Solar Cells, Wiley, London, 14, 1998.
- [6] J. Ferber, et al. Solar Energy Mat. Sol. Cells **53**, 29 (1998).
- [7] T. Oda, et al. Solar Energy Mat. Sol. Cells **90**, 2696 (2006).
- [8] G. Smestad, et al. Solar Energy Mat. **32**, 259 (1994).
- [9] A. Jungel, S. Tang, Applied Numerical Mathematics **56**(7), 899 (2006).
- [10] W. Shockley, W. T. Read Jr., Phys. Rev. **87**(3), 836 (1952).
- [11] M. Paulescu, et al. [Nanostructured Photovoltaic cells], West University of Timisoara Publ. House, 2007.
- [12] A. Sadao, [Properties of Group – IV, III-V and II-VI Semiconductors], Wiley Publisher, Chichester, 2005.
- [13] M. Paulescu, P. Gravila, E. Tulcan-Paulescu, Scientific Bulletin of the „POLITEHNICA” University of Timisoara, **53**(66), 114 (2007).
- [14] M. Paulescu, E. Tulcan-Paulescu, Modern Physics Letters B **19**,447 (2005).
- [15] L. Fara, R. M. Mitroi, V. Iancu, G. Noaje, G. Milesco, Modelling and numerical simulation of nanostructured Solar Cells **2**, Punct Publ. House, Bucharest, 2008.
- [16] L. Fara, R. M. Mitroi, V. Iancu, Proceedings of International Workshop PVTrends, Bucharest, (2008).